Plasma Chem Plasma Process (2012) 32:949–957
DOI 10.1007/s11090-012-9389-5

ORIGINAL PAPER

Highly Effective Inactivation of *Pseudomonas* sp HB1 in Water By Atmospheric Pressure Microplasma Jet Array

Xianhui Zhang · Dongping Liu · Hongzhe Wang · Linying Liu · Songbai Wang · Si-ze Yang

Received: 12 March 2012 / Accepted: 30 May 2012 / Published online: 10 June 2012

Abstract By using an atmospheric pressure microplasma jet array device driven by a.c. voltage with repetition rate of several kilohertz, we were able to inactivate the resistant *Pseudomonas* sp HB1 cells in aqueous solution. Measurements showed that all *Pseudomonas* sp. cells in a suspension of 80 mL with the concentration of $\sim 10^8$ CFU (Colony-Forming Units) were killed within a treatment time of 6 min. Rather than O radicals, OH radicals or charged species were supposed to play the most important role in the plasma inactivation process by this method. This design can provide an effective mode of killing the resistant microorganism in water.

Keywords Microplasma jet array · Dielectric barrier discharge (DBD) plasma · *Pseudomonas* sp HB1 cells · Inactivation

Introduction

The inactivation of microorganisms in water and the removal of biological hazardous contaminants are generally of great interest for both developing and developed countries. Cold plasmas operating at atmospheric pressure contain a variety of microbicidal agents, such as charged species, radicals, ultraviolet (UV) light, excited molecules, and have been successfully used for microbial decontamination [1–4]. However, so far there are insufficient reports about atmospheric pressure cold plasma inactivation of microorganisms under aqueous environment [5–7]. The major difficulties one encounters are: (1) the difficulty to form a stable and uniform cold plasma under aqueous environment. The

X. Zhang · D. Liu · H. Wang · L. Liu · S. Wang · S. Yang
Fujian Key Laboratory for Plasma and Magnetic Resonance, Department of Electric Science, School of Physics and Mechanical & Electrical Engineering, Xiamen University, Xiamen 361005, Fujian, People's Republic of China

D. Liu (✉)
Liaoning Key Lab of Optoelectronic Films and Materials, School of Physics and Materials Engineering, Dalian Nationalities University, Dalian 116600, People's Republic of China
e-mail: Dongping.liu@dlnu.edu.cn

characteristics of aqueous solution in direct contact with gas-phase plasmas, such as its conductivity can greatly alter the stability and uniformity of atmospheric cold plasmas. (2) the need to maintain the high chemical reaction efficiency of plasma-activated species in water. Before they flow into the aqueous solution, these short-lived and very active species from atmospheric plasmas quench due to the frequent collisions in the gas phase.

Pseudomonas has this ability to metabolise a variety of diverse nutrients and thrive under harsh conditions as a result of their hard cell wall that contains porins. The resistant *Pseudomonas* can cause food spoilage [8–10]. In this study, we report a hollow-fiber based microplasma array device for generating atmospheric microplasma jets in water. The microplasma array device running with He/O_2 mixtures has been successfully utilized for the plasma inactivation of *Pseudomonas* sp. (*Pseudomonas* sp HB1) cells in aqueous solution. The inactivation of *Pseudomonas* sp. cells is evaluated via colony forming unit (CFU) count on Petri dish, and atmospheric microplasma jets are characterized using I–V and optical emission measurements.

Experimental

Plasma Reactor and Multi-glow Mode Discharge

Different with the traditional single-jet configuration where the dielectric tubes of barrier discharges are generally several millimeters in diameter [11–13]. We use microns-thick and hollow quartz fibers as the dielectric tubes, through which to flow the feed gas. Figure 1a shows the schematic of the 6 × 6 microplasma jet array housed in a 0.2 L (45 × 52 × 80 mm) glass container. The inner and outer diameters of the hollow quartz fibers are 250 μm and 1,000 μm, respectively. The tungsten wires (100 μm in diameter) are inserted into these hollow fibers and act as the high-voltage electrodes of microplasma jets. The separation between the ends of tungsten wires and hollow quartz fibers is 1.2 cm. The O_2/He gases with their total flow rate of 2.2 standard litre per minute (SLM) are fed into these hollow quartz fibers. The aqueous solution containing *Pseudomonas* sp. cells acts as the grounded electrode. The power supply is capable of supplying bipolar a.c. output with peak-to-peak voltage (V_{PP}) of 0–30 kV at an a.c. frequency of 10 kHz. Microplasma jets are formed inside the hollow cores of quartz fibers near their ends. Applied voltage and discharge current are simultaneously measured using a Tektronix 2040 digital oscilloscope with a high-voltage (H.V.) probe and a Tektronix P2220 current probe. The discharge current was obtained by measuring the voltage over a small resistor (40 Ω), connected in series to ground. Measurements for the charges across this capacitor and the applied voltage across the discharge chamber result in a Lissajous figure, which was used to calculate the discharge power [14]. The discharge power can increase from 0 to about 80 W when V_{PP} is varied from 0 to 30 kV. Optical emission spectra (OES) are obtained by using a SpectraPro-750i monochromator (Acton Research Corporation) with its resolution of 0.05 nm in the wavelength range of 200–800 nm. Figure 1b shows the photograph of well-aligned He microplasma jets obtained at $V_{PP} = 4$ kV. Clearly, the microplasmas are generated inside the hollow cores of quartz fibers near their ends. The microplasma jet is formed in the vicinity of the end of each quartz fiber. A great number of microbubbles flow through the aqueous solution containing *Pseudomonas* sp. cells. Microbubbles as a part of the microplasma jet can contain a variety of microbicidal active agents, including short-lived species, such as charged species (electrons or ions) and reactive radicals. When V_{PP} is larger than 4 kV, the strong discharge can be produced between the tungsten wires and

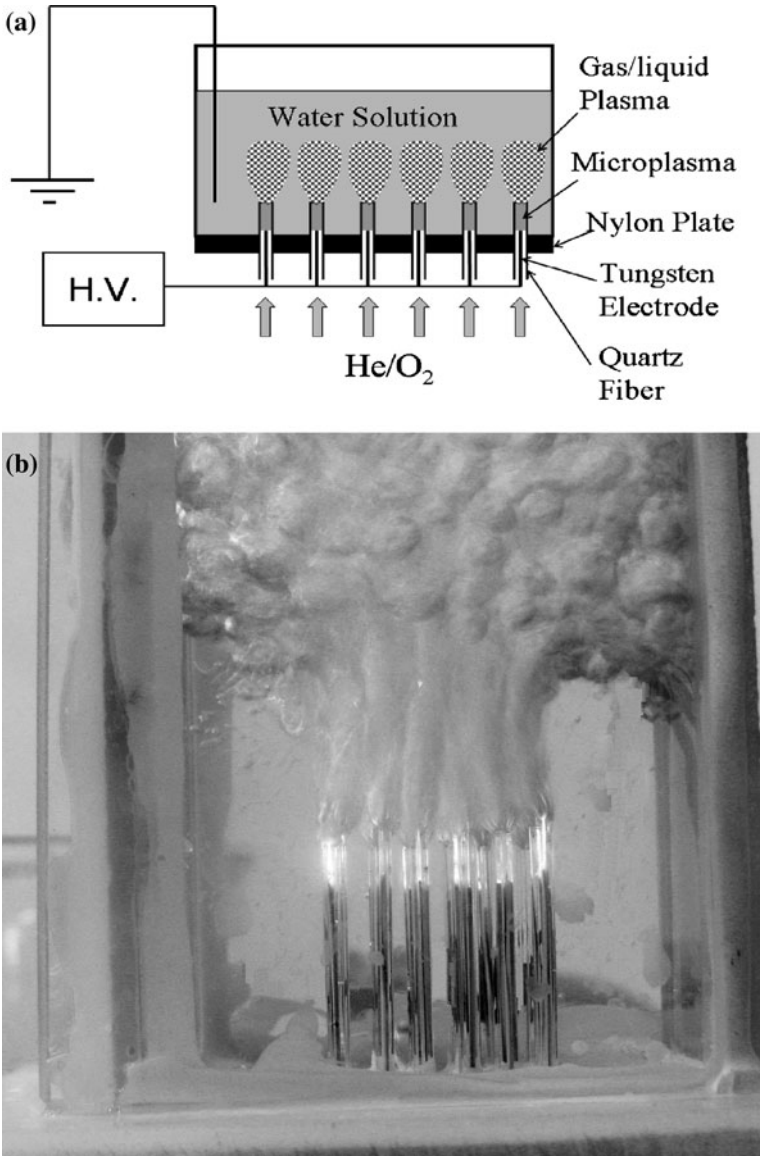

Fig. 1 **a** *Schematic drawing* of the microplasma jet array generated in aqueous solution; **b**The photograph of atmospheric helium microplasma jet array formed in aqueous solution at $V_{PP} = 16$ kV

the aqueous solution, resulting in a rapid increase in the temperature of the aqueous solution. When V_{PP} is smaller than 3–4 kV, the microplasma jets are getting much weak due to an insufficient power density. These plasma-activated species are in direct contact with the aqueous solution. This design can lead to an obvious increase in the contact area of microplasma jets with the aqueous solution, thus an improvement in the chemical reaction efficiency of plasma-activated species. The flow rate of the feed gas lower than 1.5 SLM may result in the direct contact between the tungsten wires and aqueous solution, thus the unstable microdischarges in the vicinity of the tungsten wires.

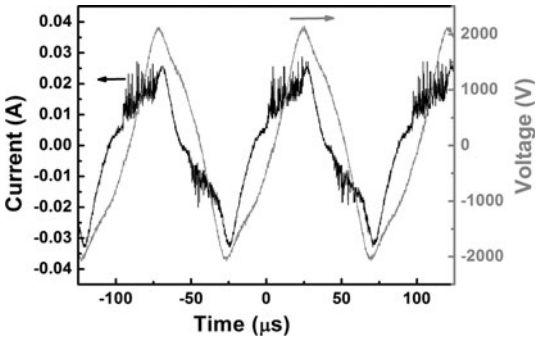

Fig. 2 The applied voltage and the total current of the microplasma jets obtained using He as the feed gas at $V_{PP} = 4$ kV

Figure 2 shows the temporal characters of the applied voltage and the total current of the atmospheric microplasma jets obtained using He as the feed gas at $V_{PP} = 4$ kV. The multi-peak appearance of the current waveform is well consistent with the previous reports [15–17]. This suggests that atmospheric dielectric barrier discharge with "multi-glow mode" [18] be generated inside the hollow-core fibers near their ends, and the microplasma jets be formed in the vicinity of the ends of hollow-core fibers. The total current appears as a discharge current superimposed onto a displacement current [15]. The discharge current stands for the effective gas breakdown, and has much shorter duration than the period of applied voltage. In the designs reported previously [7, 16, 19, 20], atmospheric cold plasma jet devices typically consist of a H.V. needle electrode and a dielectric tube. The dielectric tube is generally wrapped with the grounded metal electrode. These designs show the well consistence with the electrode configuration of dielectric barrier discharges. These devices may be used to generate the atmospheric plasma jets when the He or Ar gas is fed into the dielectric tube. In this present design, the aqueous solution surrounding the quartz fibers acts as the grounded electrode. The barrier discharge configuration consists of H.V. tungsten wires, quartz fibers, and the aqueous solution. The pulsed discharge current is formed due to the charge accumulation on the inner surfaces of hollow-core quartz fibers. The surface charges create an electric potential that opposes the applied voltage and, as a result, limit the discharge current and prevent the glow-to-arc transition [15]. The plasma density of microjets can be greatly improved due to an increase in the discharge current.

Analytical Methods

A single colony of *Pseudomonas* sp. was inoculated into the 4 mL Zobell 2216E liquid medium (Bactopeptone: 5 g/L, Yeast powder: 1 g/L, KH_2PO_4: 4 mL/L, $FeSO_4$: 2 mL/L, PH value: 7.6–7.8), and cultivated into the exponential phase with the rotation speed of 150 rpm at 28 °C. Then, 3.6 mL cultures was transferred to another 360 mL 2216E and fostered to obtain more cultures. 80 mL: of the cultures containing *Pseudomonas* sp. concentration of 2.5×10^8 CFU/mL was treated by using the atmospheric He or O_2/He microplasma jets. Then, the treated cultures was diluted according to a series of gradient using distilled water, from 10^{-1} to 10^{-6}, separately, while the untreated one was used as the control. For each dilution, we set three parallels. Then the bacterial samples were inoculated on the standard Petri dishes 9 cm in diameter containing approximately 15 mL semisolid 2216E. The static cultivation was kept at 28 °C for 24 h.

Figure 3 shows the photographs of *Pseudomonas* sp. samples (1) from the untreated cultures; (2) treated by using the 2 % O_2 + 98 % He microplasmas within the treatment

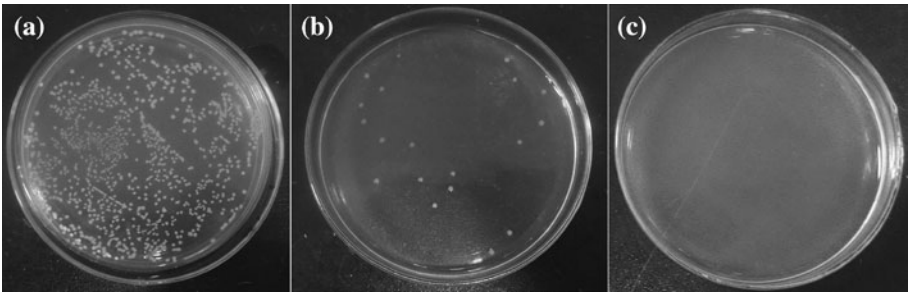

Fig. 3 *Photographs* of *Pseudomonas* sp. samples (**a**) from the untreated cultures; (**b**) treated by using the 2 % O_2 + 98 % He microplasma jets within the treatment time of 4 min.; (**c**) treated by using the 2 % O_2 + 98 % He microplasma jets within the treatment time of 6 min

time of 4 min.; (3) treated by using the 2 % O_2 + 98 % He microplasmas within the treatment time of 6 min. Measurement shows that the temperature of the cultures is lower than 35 °C within the treatment time of 10 min, and has no obvious effect on the survival efficiency of *Pseudomonas* sp. cells. This plasma treatment results in a rapid inactivation of *Pseudomonas* sp. cells in the cultures. The atmospheric O_2/He microplasmas almost killed all the *Pseudomonas* sp. cells within the treatment time of 6 min. The *Pseudomonas* sp. concentration of the cultures diluted to 10^{-6} as a function of processing time is plotted in Fig. 4. Both the processing time and O_2/He ratios have a significant effect on the survival efficiency of *Pseudomonas* sp. cells. Increasing the treatment time to 5–10 min lead to a rapid reduction in the concentration of *Pseudomonas* sp. cells in the aqueous solution. The He plasma containing 2 % O_2 is more effective in killing *Pseudomonas* sp. cells and its disinfection efficiency reaches as high as 99 % within a treatment time of 4 min. The plasma inactivation measurements were also performed when the *Pseudomonas* sp. concentration was varied from 268 × 10^5 CFU/mL to 86 × 10^8 CFU/mL. The plasma treatment with the treatment time of 5–7 min by the 2 % O_2 + 98 % He microplasmas can result in the >97 % disinfection efficiency of the *Pseudomonas* sp. cells contained in the 268 × 10^5–86 × 10^8 CFU/mL suspensions.

Results and Discussion

OES Spectra of Microplasma Jets

The typical OES spectra of these microplasma jets obtained using 100 % He or 2 % O_2 + 98 % He as the feed gas are shown in Fig. 5a, b, respectively. The major helium emission lines observed in both 100 % He and 2 % O_2 + 98 % He plasmas are from transitions of 2^3P–7^3D at 371 nm, 2^1S–3^1P at 501 nm, 2^3P–3^3D at 587 nm, 2^1P–3^1D at 667 nm, 2^3P–3^3S at 706 nm, and 2^1P–3^1S at 728 nm [21, 22]. He* atoms from the microplasma jets are mainly formed due to the collisions of energetic electrons with He atoms [23, 24]. Emissions at 316 and 357 nm from N_2 second positive system ($C^3\Pi_u$–$B^3\Pi_g$) and at 656 nm from Hα were also clearly observed. The N_2* molecules from the microplasma jets are mainly produced via the energetic collisions of electrons with N_2 molecules (e + N_2 ($X^2\Sigma_g^+$)→e + N_2 ($C^3\Pi$, $B^3\Pi$)) or excited by the long lived helium metastable

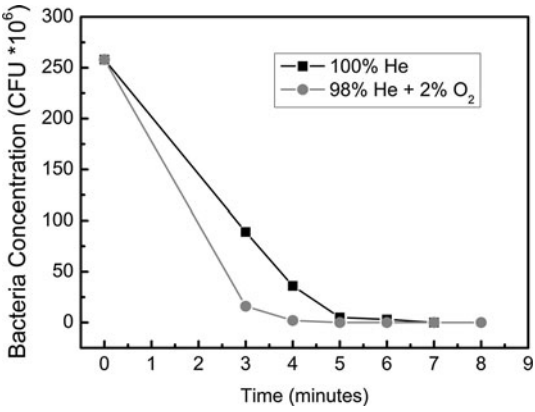

Fig. 4 The *Pseudomonas* sp. concentration of the cultures diluted to 10^{-6} as a function of processing time

(19.8 eV) via the Penning ionization process ($He(2^3) + N_2$ ($X^2\Sigma_g^+$)→$He + N_2$ ($C^3\Pi$, $B^3\Pi$)) [23–25]. The strong OH emissions from both 100 % He and 2 % O_2 + 98 % He plasmas are assigned to transitions of $A^2\Sigma^+$–$X^2\Pi$ ($\Delta v = 1$) at 285 nm and $A^2\Sigma^+$–$X^2\Pi$ ($\Delta v = 0$) at 309 nm.[22] Since water vapour molecules can diffuse into the microplasma jets, OH and H radicals can be formed by the Penning ionization process of water vapour ($He(2^3) + H_2O \rightarrow He + H + OH$) or by electronic impact dissociation ($H_2O + e^- \rightarrow H + OH + e^-$). The O emission at 777 nm observed for the 2 % O_2 + 98 % He plasma was assigned to the transition of $2s^22p^33$ s–$2s^22p^33p$. In the He microplasma jets containing a small amount of O_2, both energetic electrons and excited He* can ionize O_2 molecules [23–25], which can be responsible for the formation of O radicals.

Plasma-Activated Species for Inactivation of Microorganism

So far, all the plasma induced species, such as charged species (electrons and ions), reactive species, UV photons (generated due to the radiation of excited species) were supposed to play the role in the sterilization process by low temperature plasmas [26–29] In this method, the aqueous solution containing *Pseudomonas* sp. cells was subject to all possible agents generated by the plasmas, including charged particles, reactive neutrals, and UV photons. UV radiation in the 200–300 nm wavelength range with doses of several milliwatt-seconds per square centimeter are known to cause lethal damage to cells [30]. However, the atmospheric-pressure plasma jet, as the most effective type of cold plasmas for sterilization, usually produces very little UV [4]. It is believed that UV does not play a major role in the inactivation process by atmospheric-pressure cold plasmas [4, 12, 27, 31]. Charged particles can play a significant role in the rupture of the outer membrane of bacterial cells [4, 28]. The electrostatic force caused by charge accumulation on the outer surface of the cell membrane could overcome the tensile of the membrane and cause its rupture. In this study, the microplasma jets are in direct contact with the *Pseudomonas* sp. cells in the aqueous solution. These short-lived charges can diffuse into the aqueous solution before they recombine with other species during frequent collisions. Especially, the plasma sheath formed near the plasma/liquid interface can cause the potential difference between the gas-phase plasma and the *Pseudomonas* sp. cells from this interface. Therefore, the charge accumulation on the outer surface of *Pseudomonas* sp. cells may occur due to the existence of plasma sheath, which can rapidly cause their ruptures.

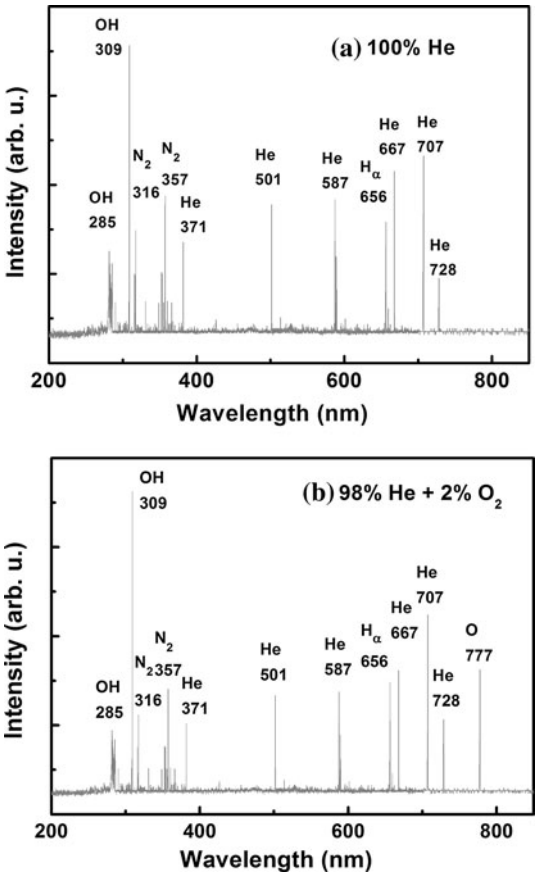

Fig. 5 The typical OES spectra of these microplasma jets obtained using (**a**) 100 % He and (**b**) 2 % O_2 + 98 % He as the feed gas in aqueous solution

Among various plasma-activated neutrals, O and OH radicals were supposed to play a crucial role in the plasma inactivation of microorganism [7, 32, 33]. Especially, O radicals were believed to play the most important role in this inactivation process [1, 20, 34, 35]. These reactive species have strong oxidative effects on the outer structures of cells. However, no emission from O radicals was observed from the He plasma in this present study. Strong emission from OH radicals indicates that OH radicals can be very effective in killing the resistant *Pseudomonas* sp. cells in aqueous solution. In deed, OH radicals with oxidation potential of 2.8 V was supposed to be most reactive and toxic among all reactive oxygen species (ROS) [7]. OH radicals can attack unsaturated fatty acids in the cell membranes [31]. The unsaturated fatty acids give the membrane a gel-like nature, and the membrane containing unsaturated fatty acids acts as a barrier against the transport of ions and polar compounds in and out of the cells. The He plasma containing a small amount of O_2 exhibits more effective inactivation of *Pseudomonas* sp. cells in aqueous solution, which can be related to the generation of O radicals in the microplasma jets. Protein molecules, which are basically linear chains of amino acids, are susceptible to oxidation by the O radicals very active during chemical reaction [27]. Proteins also play the role of gateways that control the passage of various macromolecules in and out of cells. In deed, OH radicals can be formed by the reaction of excited O radicals with water vapour ($H_2O + O^* \rightarrow 2OH$) [7, 36, 37]. This process may lead to an increase in the concentration

of OH in aqueous solution, thus improve the inactivation efficiency of the resistant *Pseudomonas* sp. cells in aqueous solution.

Conclusions

The hollow-fibers based microplasma array device may help to overcome problems in the cold plasma inactivation of microorganisms from aqueous solution. In this design, the short-lived species, such as very active radicals and charge species from microplasma jets can be in direct contact with the microorganisms in aqueous solution, which can result in the highly effective inactivation of resistant *Pseudomonas* sp. cells. Analysis indicates that OH radicals and charged species play the crucial roles in the plasma inactivation of *Pseudomonas* sp. cells by this study.

References

1. Perni S, Shama G, Hobman JL, Lund PA, Kershaw CJ, Hidalgo-Arroya GA, Penn CW, Deng XT, Walsh JL, Kong MG (2007) Appl Phys Lett 90:073902
2. Ehlbeck J, Schnabel U, Polak M, Winter J, von Woedtke T, Brandenburg R, von dem Hagen T, Weltmann K-D (2011) J Phys D Appl Phys 44:013002
3. Lu X, Xiong Z, Zhao F, Xian Y, Xiong Q, Gong W, Zou C, Jiang Z, Pan Y (2009) Appl Phys Lett 95:181501
4. Laroussi M (2009) IEEE Transact Plasma Sci 37:714–725
5. Sakiyama Y, Tomai T, Miyano M, Graves DB (2009) Appl Phys Lett 94:161501
6. Nishioka H, Saito H, Watanabe T (2009) Thin Solid Films 518:924–928
7. Bai N, Sun P, Zhou H, Wu H, Wang R, Liu F, Zhu W, Lopez JL, Zhang J, Fang J (2011) Plasma Process Polym 8:424–431
8. Pereira JN, Morgan ME (1957) J Bacteriol 74:710–713
9. Levine M, Anderson DQ (1932) J Bacteriol 23:337–347
10. Gennari M, Dragotto F (1992) J Appl Bacteriol 72:281–295
11. Kolb JF, Mohamed AAH, Price RO, Swanson RJ, Bowman A, Chiavarini RL, Stacey M, Schoenbach KH (2008) Appl Phys Lett 92:241501–245562
12. Lu X, Ye T, Cao Y, Sun Z, Xiong Q, Tang Z, Xiong Z, Hu J, Jiang Z, Pan Y (2008) J Appl Phys 104:053309
13. Walsh JL, Kong MG (2008) Appl Phys Lett 93:111501
14. De Geyter N, Morent R, Gengembre L, Leys C, Payen E, Vlierberghe SV, Schacht E (2008) Plasma Chem Plasma Process 28:289–300
15. Lee HW, Nam SH, Mohamed A-AH, Kim GC, Lee JK (2010) Plasma Process Polym 7:274–280
16. Chen L, Zhao P, Shu X, Shen J, Meng Y (2010) Phys Plasmas 17:083502
17. Song Y, Liu D, Ji L, Wang W, Niu J, Zhang X (2012) IEEE Transact Plasma Sci 99:1–5
18. Sublet A, Ding C, Dorier J-L, Hollenstein C, Fayet P, Coursimault F (2006) Plasma Sources Sci Technol 15:627–634
19. Jiang N, Ji A, Cao Z (2010) J Appl Phys 108:033302
20. Léveillé V, Coulombe S (2005) Plasma Sources Sci Technol 14:467–476
21. Yu Ralchenko, Kramida AE, Reader J, NIST ASD Team (2008) NIST Atomic Spectra Database (version 3.1.5), [Online]. Available: http://www.nist.gov/pml/data/asd.cfm 2009, July 21. National Institute of Standards and Technology, Gaithers-burg, MD
22. Sarani A, Nikiforov AYu, Leys C (2010) Phys Plasmas 17:063504
23. Zhu W, Li Q, Zhu X, Pu Y (2009) J Phys D Appl Phys 42:202002
24. Golubovskii YB, Maiorov VA, Behnke J, Behnke JF (2003) J Phys D Appl Phys 36:39–49
25. Sublet A, Ding C, Dorier J-L, Hollenstein C, Fayet P, Coursimault F (2006) Plasma Source Sci Technol 15:627–634
26. Wang D, Zhao D, Feng K, Zhang X, Liu D, Yang S (2011) Appl Phys Lett 98:161501
27. Laroussi M (2005) Plasma Process Polym 2:391–400
28. Stoffells E, Sakiyama Y, Graves DB (2008) IEEE Trans Plasma Sci 36:1441–1457

29. Kong MG, Kroesen G, Morfill G, Nosenko T, Shimizu T, van Dijk J, Zimmermann JL (2009) New J Phys 11:115012
30. Norman A (1954) J Cell Comp Physiol 44:1–10
31. Laroussi M, Leipold F (2004) Int J Mass Spectrom 233:81–86
32. Sun P, Sun Y, Wu H, Zhu W, Lopez JL, Liu W, Zhang J, Li R, Fang J (2011) Appl Phys Lett 98:021501
33. Goree J, Liu B, Drake D (2006) J Phys D Appl Phys 39:3479–3486
34. O'Connell D, Cox LJ, Hyland WB, McMahon SJ, Reuter S, Graham WG, Gans T, Currell FJ (2011) thensmjdkdjdkdkd. Appl Phys Lett 98:043701
35. Lim J-P, Uhm HS, Li S-Z (2007) Phys Plasma 14:093504
36. Freeman BA, Crapo JD (1982) Lab Invest 47:412–426
37. Dreher D, Junod AF (1996) Eur J Cancer 32(1):30–38